DETECTION OF AUDIBLE RESONANCES

Ivo Mateljan, Heinrich Weber*, Ante Doric**

Faculty of electrical engineering, R. Boskovica bb, 21000 Split (ivo.mateljan@fesb.hr), *CTC, Langelohstraße 134, D-22549 Hamburg (ctc@ctc-dr-weber.de), **Croatian Radio Split, 21000 Split (ante.doric@hrt.hr)

Abstract: *The paper discusses the problem of the detection of audible resonances. The basic psychoacoustic researches have shown that the threshold of resonance detection can be classified by resonance level and Q-factor. In this work a third criteria is introduced. It is the energy of the resonance. By analyzing the influence of resonances on the frequency response and group delay, it is shown that it is almost impossible to detect resonances that are near the threshold of audibility. Finally, three common techniques for resonance detection are compared: the cumulative spectral decay, the shaped sine burst decay and the transfer function pole–zero identification. In the conclusion suggestions for the use of the particular method are given.*

Key words: audible resonances, cumulative spectral decay, burst decay, pole-zero identification

1. INTRODUCTION

Physical sources of resonances are structural vibrations and standing waves. Delayed (reflected) waves are not resonances, but if they form standing waves or if they excite additional structural vibrations they are called delayed resonances.

Detection and perceptual evaluation of loudspeaker resonances is of prime importance in loudspeaker design. Resonances represent the main cause of unpleasant loudspeaker sound. They affect three main loudspeaker characteristics: tonal balance, modulation dynamics and object perception. The change in tonal balance is usually called coloration. The change in object perception is usually described as boxy sound. The change in modulation depth is usually described as change in transparency and dynamics. Opposite to unwanted effects in sound reproduction resonances have a specific role in sound generation in musical instruments. This paper considers detection of resonances in sound reproduction systems only.

In the next section a perceptual model for the evaluation of loudspeaker resonances is presented. It is based on the well known works of Fryer [1], Floyd and Olive [2]. They analysed the threshold of audibility of resonances and showed that steady state amplitude and Q-factor of resonances are key factors in determining the threshold of resonance audibility. By using their results a simple energetic model of resonance detection is presented. It was shown that objective detection of audible resonances is very difficult as some audible resonances make very small, almost non-measurable changes to audio signals.

The paper discusses three advanced measurement methods for the detection of resonances:
1) Cumulative spectral decay, as special case of the Short Time Fourier Transform method,
2) Burst decay envelope as a case of continuous wavelet transform with optimal time-frequency bandwidth,
3) Pole-zero identification.

Beside using these advanced techniques, resonances can be partly detected from classical measurement curves: frequency response, group delay, loudspeaker input impedance and harmonic distortions. Simple, non-quantified resonance detection is possible by noting changes in monotonicity of these curves.

For the analyzed resonance detection methods key properties are:
1) visualization of resonances decay pattern with optimal time-bandwidth resolution,
2) estimation of basic resonance parameters (Q-factor, resonance frequency and resonance level),
3) discrimination of resonances from reflections.

The conclusion gives directions for applicability of these methods in acoustical instrumentation.

2. PERCEPTUAL MODEL FOR RESONANCE DETECTION

The works of Fryer [1], Floyd and Olive [2] give a very simple perceptual model for the detection of resonances. They analyzed the threshold of audibility of a band pass filtered signal that was added to original signal. The filter had a characteristic of a first order resonator with known Q-factor, resonant frequency f_r and steady state gain level L_r. The results of Fryer are shown in Figure 1.
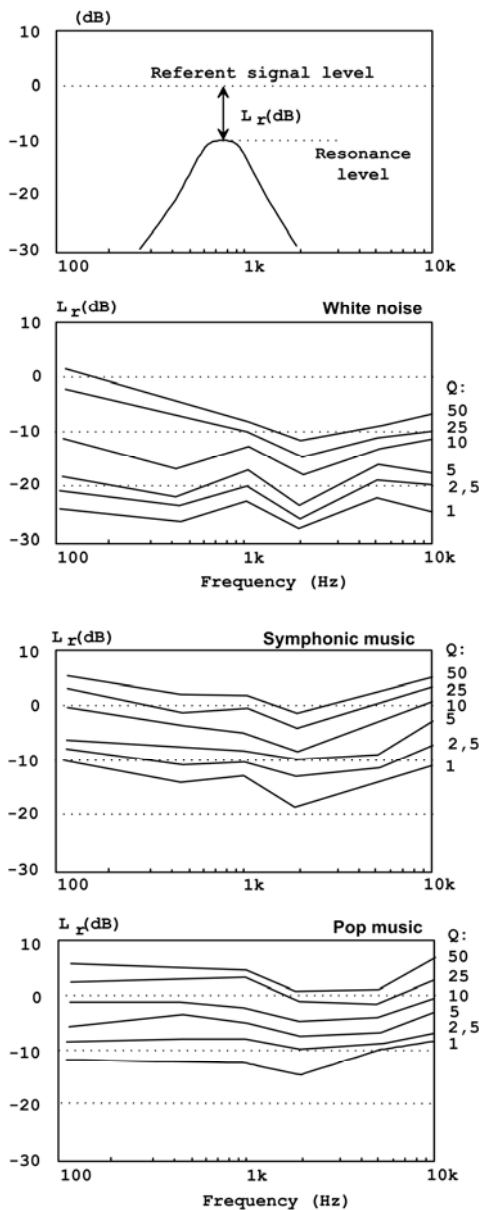

Fig. 1. Results for the threshold of resonance audibility (range of Q from 1 to 50) after Fryer [1]

Floyd and Olive [2] got almost the same results for threshold levels as in Fryer's work (within ±3dB). From their work, we find following important conclusions:

1. The perceptual resonance threshold level is lowest if the test signal is white or pink noise.
2. The lowest threshold level is for Q=1 and depends on frequency, and has a value from -29dB to -23dB.
3. The threshold level is proportional to Q-factor, which means that resonances with a low Q are more audible than with a high Q. Doubling the resonance Q-factor raises the threshold of resonances audibility for 3dB.
4. If the resonance signal is delayed for more than 1ms the perceptual threshold is becoming lower for transient signals, or becoming higher for complex signals and noise. For example, if resonance is delayed 20ms the threshold for transient signal is being lowered to -40dB.
5. Resonances with Q>50 are more audible with transient signals while resonances with Q<10 are more audible with continuous complex signals.
6. Although there is a slight frequency dependence of the threshold level it is practically independent from frequency for Q<10. Differences in threshold levels are less than ±5dB.
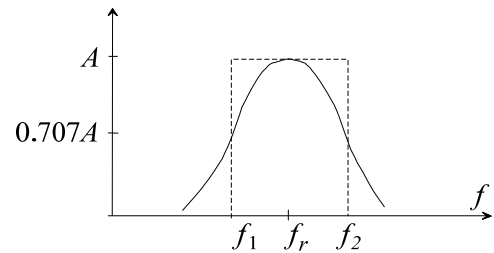

Fig. 2. Resonant filter with gain A, resonant frequency f_r and -3dB bandwidth $\Delta f = f_2 - f_1$

One question arises from these conclusions and needs additional explanation: Why low-Q resonances are more audible than high-Q resonance? The explanation can be given from famous masking experiments [3] where it was shown that the loudness of a narrowband signal is proportional to signal energy.

The Parsavel theorem states that the wideband signal energy that passes through resonant filter is equal to the integral of the signal power spectral density. For the resonant filter that is shown in Fig. 2 the energy of wideband noise or transient signal is equal to:

$$E = \int_{f_1}^{f_2} A^2 df = A^2 (f_2 - f_1) = A^2 \frac{f_r}{Q} \qquad (1)$$

where: $Q = f_r / (f_2 - f_1)$.

Expression (1) shows that the energy of wideband signals, that passes a resonant filter on frequency f_r, is inversely proportional to the filter Q-factor. By doubling the Q-factor the energy is being lowered 3dB. This

explains Floyd's second conclusion that doubling the resonance Q-factor raises the threshold of audibility for 3dB. Low-Q resonances span over several critical bands so their loudness can be even larger than loudness of high-Q resonances that are localized inside the same critical band.

3. FREQUENCY RESPONSE WITH RESONANCES

It is interesting to analyze how a single resonance changes frequency response of the system. We use a additive model of the system transfer function $H(s)$. It is composed out of the resonant part $H_r(s)$ and the non resonant part $H'(s)$.

$$H(s) = H_r(s) + H'(s) \qquad (2)$$

The resonant part of the transfer function can be described with pairs of complex conjugate poles $s_p = -\alpha \pm j\beta$. Partial fractional expansion of those poles that have complex residuum amplitude $R = r \pm jv$, have the following forms:

$$H_r(s) = \frac{R}{s + \alpha + j\beta} + \frac{R^*}{s + \alpha - j\beta} \qquad (3)$$

$$H_r(s) = 2r \frac{s + \left(\alpha - \beta \frac{v}{r}\right)}{s^2 + s \frac{\omega_n}{Q} + \omega_n^2} \qquad (4)$$

In these equations the resonant behavior is described completely by three parameters:

1. Natural resonant frequency: $\omega_n = \left(\alpha^2 + \beta^2\right)^{-1/2}$,
2. Q-factor: $Q = \omega_n / 2\alpha$,
3. ΔL – difference of resonator maximum magnitude level and system magnitude level. If ΔL is below the value of perceptual threshold L_r, the resonance is not audible.

This means that if we estimate values of poles and zeros of the transfer function, a partial fractional expansion of the transfer function gives us all the necessary information for the perceptual evaluation of resonances. This will be discussed more in detail in section 7.

It is interesting to analyse the contribution of resonances that are close to the threshold of audibility to the frequency response. Three cases, for Q = 1, 3, 10, are shown in Fig. 3. The least contribution to the frequency response is for Q=1. The maximum change of magnitude level is less than 0,8dB, change of phase is less than 2º and change of group delay is less than 0,05ms. The conclusion is that it is very difficult or almost impossible to detect these low-Q resonances from frequency response curves. Differences from the ideal case are less than the ripple of frequency response of good measuring microphones.
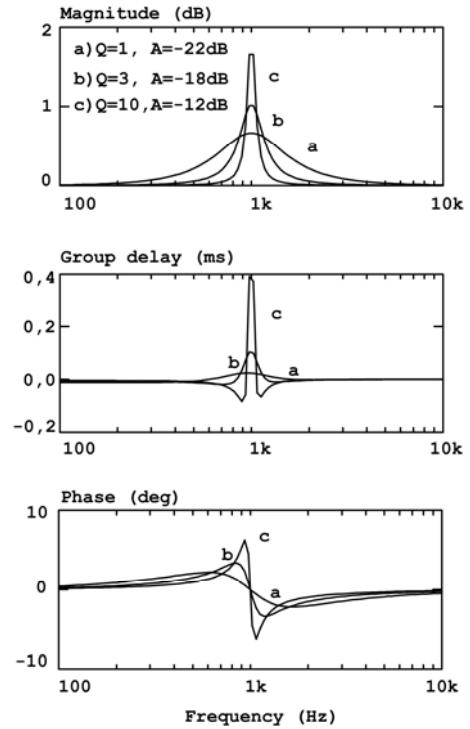

Fig. 3. Contribution to frequency response of resonances with Q = 1, 3, 10. The level of each resonance is close to the threshold of audibility.

4. DO WE NEED DAMPING?

The conclusion that resonances with a low Q-factor have a lower threshold of audibility than resonances with a high Q-factor implies the question: Does damping of resonances reduce their audibility? The answer is: yes and no, depending on how the damping is applied. Examples of both cases will be shown by analysing the resonant filter that is shown in Fig. 4.
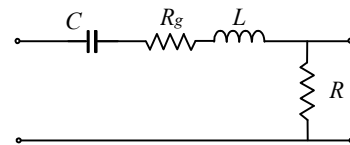

Fig. 4. Simple resonant filter (Rg is damping resistance, R is load resistance)

For the circuit in Fig. 4, that has transfer function $H_r(s)$, resonant frequency and Q-factor are:

$$\omega_n \cong \frac{1}{\sqrt{LC}}, \quad Q \cong \frac{\omega_n L}{R_g + R} \qquad (6)$$

The maximum of the transfer function magnitude is:

$$A = \left| H_r(j\omega) \right|_{max} \cong \frac{R}{R + R_g} = \frac{R}{L}\frac{Q}{\omega_n} \qquad (7)$$

The total energy transfer of the resonant filter is estimated by substituting (7) in (1). That gives the following expression:

$$E = \frac{R^2}{2\pi(R + R_g)L} = \frac{R^2}{2\pi L^2}\frac{Q}{\omega_n} . \qquad (8)$$

If we increase the damping, by increasing the resistance R_g, the Q-factor will be lowered as well as the total resonant energy transfer. This is always true if the coupling to the load is unchanged ($R=const.$), for example if we apply absorptive material in the loudspeaker box, or if we apply damping on vibrating panels.

The resonant energy transfer can be also reduced by changing the coupling to the load. If we lower the load resistance R, according to (7), Q-factor will be raised, but the energy transfer will be lower. This effect can appear if we change the coupling in horn loaded loudspeakers.

Previous examples show that a reduction of resonances can be achieved by lowering or by increasing the Q-factor. The only way to assure that damping reduces the perceptual influence of the resonance is by confirming that energy transfer due to the resonance is reduced.

5. CUMULATIVE SPECTRAL DECAY (CSD)

A waterfall plot of the time-frequency function, called Cumulative Spectral Decay (CSD), is often used in audio measurement software [4] as a primary tool for detection of resonances.

The cumulative spectral decay is defined by Bunton and Small [5] as a time-frequency function:

$$C(t,\omega) = \int_{-\infty}^{\infty} h(\tau) u_0(\tau - t) e^{-j\omega\tau} d\tau \qquad (9)$$

where $h(t)$ is the impulse response function and $u_0(t)$ is the unit step function.

Theoretically, $C(t, \omega)$ is a Fourier transform of the part of the impulse response that is defined from time $\tau = t$ to infinity, as shown in Fig. 5.
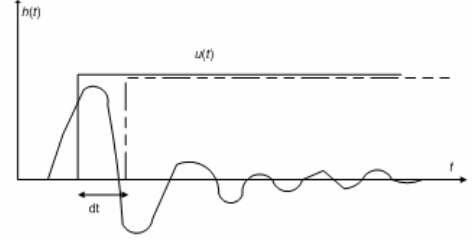

Fig. 5. Construction of the integral function of $C(t, \omega)$.

To better understand the significance of this function we multiply $C(t, \omega)$ with $e^{j\omega t}$,

$$C(t,\omega)e^{j\omega t} = \int_{-\infty}^{\infty} h(\tau) u_0(\tau - t) e^{j\omega(t-\tau)} d\tau \qquad (10)$$

The equation for imaginary part only is given by:

$$\left| C(t,\omega) \right| \sin(\omega t + \arg[C(t,\omega)]) = \int_{-\infty}^{\infty} h(\tau) u_0(\tau - t) \sin(\omega(t - \tau)) d\tau$$

The integral on the right side is a convolution of the system impulse response $h(t)$ and the excitation function

$$f(t) = u_0(-t)\sin(\omega t) \qquad (12)$$

which is a sine function that exist in time $t<0$ and being zero from $t=0$. As the linear system response to the sine function is also a sine function, we can conclude that $\left| C(t,\omega) \right|$ is an envelope of the sine function response, after the excitation has been switched off.

The repeated application of the Fourier transform, each for a part of an impulse response that is ahead in time for an interval dt, we get the time-frequency function which is usually shown as waterfall graph (Fig. 6) or as sonogram (Fig. 7).

The CSD analysis of the system impulse response has to be done by treating the impulse response as a nonstationary signal. That implies that Fourier analysis has to be applied on least possible part of the impulse response. Practically, it means that CSD has to be calculated using the Short Time Fourier Transform with a finite width of the sliding time window. Bunton and Small [2] advocated the use of the "apodizing" window, which is a type of gradually rising and falling rectangular window. Time constant of the rising and falling part is usually in the range from 0.02 to 1ms. The form of the rising and falling part of the window usually has the form of half the Blackman window.
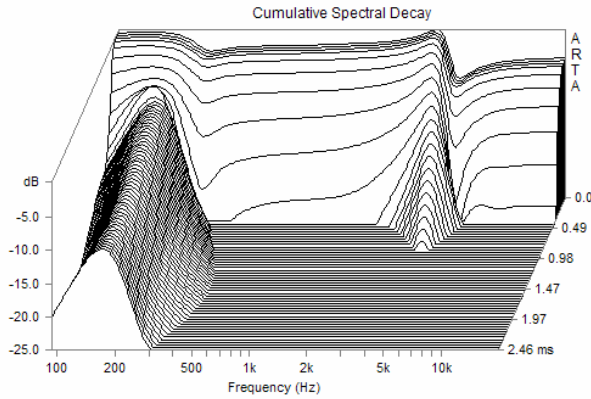
Fig. 6. CSD waterfall graph for a system with two resonances at 200Hz and 5kHz, both with Q = 4.

Two problems can be noted from CSD graphs:

1. CSD has much better resolution at higher frequency than at lower frequencies. The reason for this is that the DFT analysis has a constant bandwidth Δf.
2. Time axis of CSD graph is linear, so it is impossible to compare resonance behaviour at lower and higher frequencies with equal weight (resonances with same Q factor at lower and higher frequencies have a energy decay that lasts much longer at lower frequencies). A requirement for the replacement of time scale t in CSD graphs with period T based scale t/T arises.
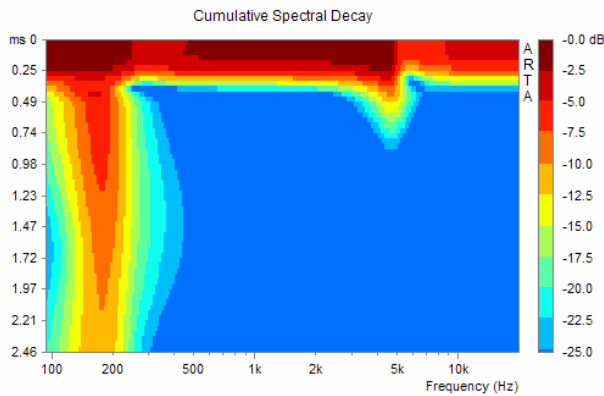

Fig. 7. CSD sonogram for system with two resonances at 200Hz and 5kHz, both with Q = 4.

The detection of resonances becomes harder if the system response contains reflections. Figure 8 shows a CSD for a impulse response of a ideal system with a single reflection that has an amplitude 10dB below the direct wave and a delay of 10.5ms. As can be seen, although the reflection is delayed 10.5ms, it obscures the waterfall plot after the 6.2 ms (as FFT size is equal 5.33ms).
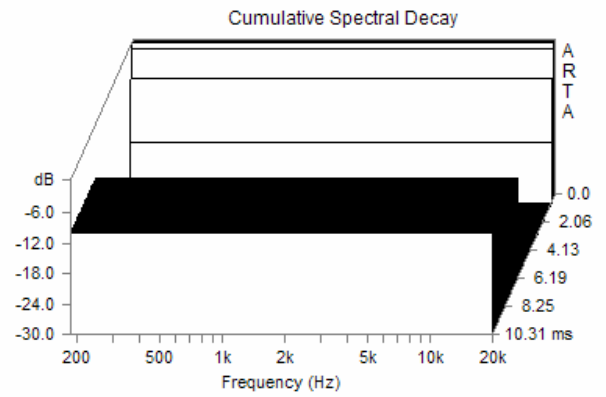

Fig. 8. CSD of an ideal system with a single reflection having a amplitude of 10dB below the direct wave and a delay of 10.5ms (FFT size is 256 samples or 5.33 ms)

One possible way to remove reflections is to apply fixed time gating (or trunctuation) of the impulse response before the onset of the reflected wave. This method causes that time-bandwidth requirement is changing as the sliding window reaches the trunctuation point. That must be taken into the account when constructing the waterfall plot – only frequency components that satisfy the time-bandwidth requirement could be shown. If the time interval of a non-trunctuated part of a impulse response in the window is T, then the lowest shown frequency component would be higher than 1/T.

5. BURST DECAY ENVELOPE

The monitoring of the shaped sine burst response is a known technique for the analysis of the transient behaviour of resonant systems [6]. A constant number of N cycles of the shaped sine burst (Fig. 9) are used to excite the measured system on a frequency f_i with a constant relative bandwidth $\Delta f/ f_i$. The envelope of the system response is monitored to give insight into the burst decay patterns. Fig. 10 and alternatively Fig. 11. shows envelopes of shaped sine bursts decay responses. A waterfall graph shows the *level* of burst response envelopes as a function of *frequency* and *number of periods of the burst sine signal* (t/T).
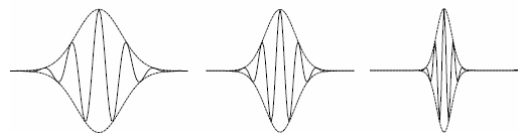

Fig. 9. Sine bursts shaped with a Gaussian window (shown as envelope). The constant number of cycles on every frequency assures a constant relative bandwidth
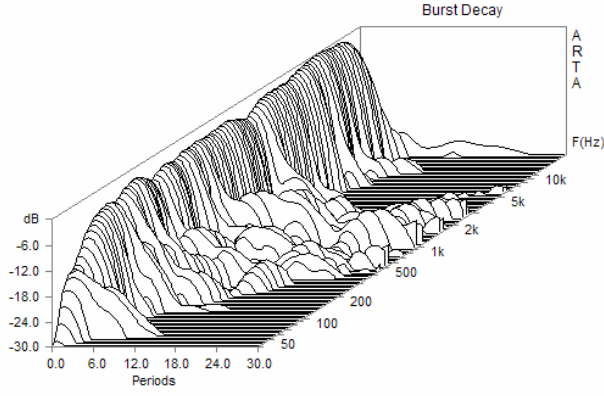
Fig. 10. Burst decay envelopes of the shaped sine burst response of a small loudspeaker

The importance of monitoring the burst response envelope in the period based time scale will be shown by analysing the response of a simple resonant circuit, which is a second order low pass filter that has a transfer function in following form:

$$H(s) = \frac{\omega_n^2}{s^2 + 2\varsigma\omega_n s + \omega_n^2} = \frac{1}{1 + s\dfrac{T}{Q} + s^2 T^2} \quad (13)$$

where ω_n is a natural resonance frequency ($T = 1/\omega_n$), ς is a damping factor and $Q = 1/(2\varsigma)$ is a Q-factor. The filter impulse response has a form of the decayed sine function:

$$h(t) = \frac{\omega_n}{\sqrt{1 - \varsigma^2}} e^{-\varsigma\omega_n t} \sin\left(\omega_n t\sqrt{1 - \varsigma^2}\right), \ t > 0 \quad (14)$$

The real energy decay appears on the frequency $\omega_0 = \omega_n\sqrt{1 - \varsigma^2}$. The system exhibits the resonance if the damping is lower than 1 ($\varsigma < 1$, $Q > 0{,}5$). In that case the response is a periodically decayed function (ω_o is real). For higher damping ($\varsigma \geq 1$, $Q \leq 0{,}5$) the response is not periodic (ω_o is imaginary).

As a result of the analysis of complex systems like loudspeakers, that have many resonances with characteristics of high pass, low pass and all-pass filters, it can be shown that all resonances have similar decay pattern expressed as envelope of the impulse response:

$$envelope\,(h(t)) = e^{-\varsigma\omega_n t}, \quad (15)$$

or in the logarithmic form:

$$\ln[envelope\,(h(t))] = -2\pi\varsigma f_n t = -\pi f_n t / Q \quad (16)$$

Last equation shows that in the graph with a period based scale ($t/T_n = tf_n$) the logarithm of the resonance burst envelope is proportional to the number of periods

with a proportionality factor equal to resonance damping. This property of the period based time scale is in accordance with results of the psycho-acoustical researches which show that human perceptual system gives similar weights to resonances with the same Q-factor on all frequencies.
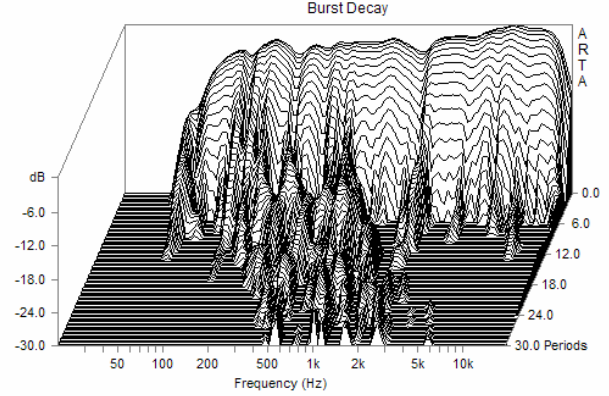

Fig. 11. Burst decay envelopes of a small loudspeaker – a waterfall view of burst decay from Fig. 10.

The system response to the shaped sine burst has two characteristic time regions: Rise time and decay time. By little more analysis it can be shown that the logarithm of the decay envelope lasts much longer than the logarithm of the rise envelope. This is the reason why we are almost exclusively interested in the monitoring of the burst decay envelope.

The direct measurement of burst decay patterns needs a lot of time, as for every frequency the sine burst response has to be generated and measured separately. A faster way to get a burst decay envelope at various frequencies is to use a measured impulse response and convolve it with a shaped sine burst signal. As a result it gives the burst response. To get the burst decay envelope a Hilbert transform can be used [7].

A more efficient estimation method is applied in the program ARTA [4]. It uses the complex Morlet wavelet analytic signal in convolution with the system impulse response. The magnitude of that response, also known as *wavelet scalogram*, represents the envelope of the shaped burst response decay.

The complex Morlet wavelet analytic signal is defined as:

$$w(t) = e^{-t^2/\tau^2} e^{j\omega_0 t} \quad (17)$$

It is just a cosine (+ sine) function modulated with a Gaussian window. The Fourier transform of the Morlet wavelet is equal to:

$$W(\omega) = e^{-(\omega-\omega_0)^2 \tau^2/4} = e^{-\left(\frac{\omega}{\omega_0}-1\right)^2 \omega_0^2 \tau^2/4} \quad (18)$$

It also has the shape of the Gaussian window. The relative 3dB bandwidth of $W(f)$ is equal to:

$$\frac{\Delta f}{f_0} = \frac{2.3548}{\omega_0 \tau} \qquad (19)$$

In acoustical measurements it is common to choose relative bandwidths of 1/3 or 1/6 octave, as it is close to the value of the bandwidth of critical bands.
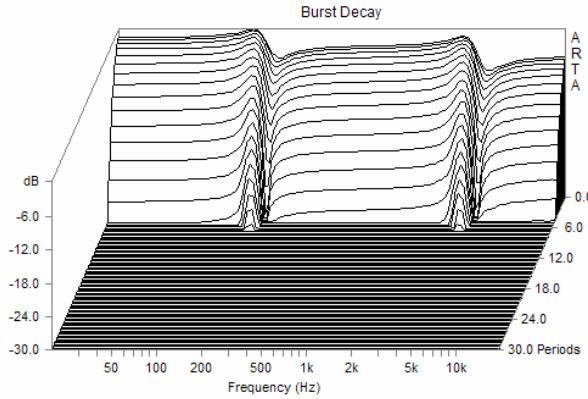

Fig. 12 Burst decay for system with two resonances at 200Hz and 5kHz, both with Q = 4.

The importance of constant relative bandwidth analysis and a period based time scale is illustrated in Fig. 12. The graph shows identical pattern for the burst decay of a system with two resonances at 200Hz and 5kHz, both with Q = 4. This is a much more perceptual relevant visualization of resonances than represented by the CSD plot in Fig. 6, as resonance with a same Q-factor show the same decay pattern.
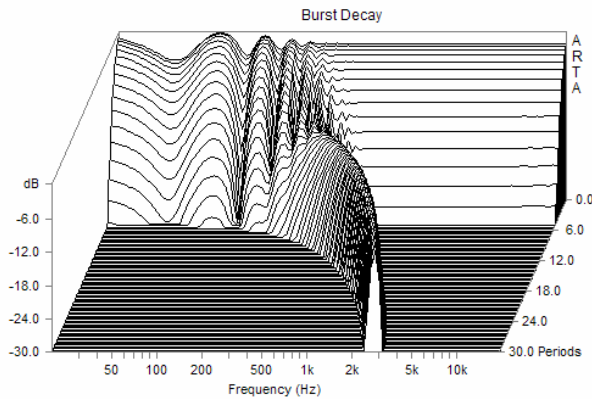

Fig. 13. Burst decay of an ideal wideband system with a single reflection

There is a problem in evaluation of resonances using burst decay envelopes if the Q-factor is lower than two, especially when system has delayed paths. In that case a period based graph shows some "unnatural" patterns. The problem is illustrated in Fig. 13. It shows the burst decay of a ideal wideband system with a single reflection. The delay of reflection is t_d=10.5ms and the amplitude is 10dB below the level of the ideal response.

The decay pattern of a delayed impulse (Fig. 13) shows a shift to the right at higher frequencies. At low

frequencies decay pattern is similar to the decay pattern of low-Q resonances. The shift of decays to the right can be explained with the following reasoning: Every reflection is localized at a number of periods (n_p) that is equal to the product of the reflection delay and a burst frequency;

$$n_p = f t_d \qquad (20)$$

At low frequencies this number is small and a decay pattern is smeared with the response of the non delayed response. At higher frequencies the delayed reflection is localized at a number of period n_p that is proportional to the frequency. That makes the shift of decay pattern to the right. This feature is good and bad. It is bad as it obscures the low-Q resonances detection on lower frequencies. It is good on higher frequencies as it separates decay pattern of reflections (which shifts to right), from decay pattern of resonances (which follows strait line on one frequency).

6. TRANSFER FUNCTION IDENTIFICATION

It will be shown that the most desirable form for resonance detection is if we can estimate the analytical form of the transfer function in the complex frequency plane. The transfer function is defined as:

$$H(s) = \frac{B(s)}{A(s)} = \frac{\sum_{i=0}^{m} b_i s^i}{\sum_{k=0}^{n} a_k s^k} = \frac{b_n}{a_m} \frac{\prod_{i=1}^{m}(s - s_{zi})}{\prod_{k=1}^{n}(s - s_{pk})} \qquad (21)$$

The transfer function $H(s)$ is the Laplace transform of the systems impulse response $h(t)$. The first form of $H(s)$ is the quotient of two polynomials $B(s)$ and $A(s)$. They are m-order and n-order power series of the complex variable s. The second form of the transfer function in Eq. (21) is the factorised form with m zeros (s_{zi}, i=0,1,..m) and n poles poles (s_{pk}, k=0,1,..n). The system frequency response $H(j\omega)$ can be obtained by substituting $j\omega$ instead of the complex variable s.

The identification of the transfer function is a process of estimating the parameters of the transfer function (21). It can be made from the measured impulse response $h_m(t)$ or the measured frequency response $H_m(j\omega)$. The problem is to find the system order m,n and coefficients b_i and a_k, that give the best fit of $H(j\omega)$ to $H_m(j\omega)$. Mathematically, this problem is defined as nonlinear least square estimation (NLSE) problem, where the following error function needs to be minimzed:

$$E = \sum_{\omega=\omega_1}^{\omega_2} \left| H_m(\omega) - \frac{B(\omega)}{A(\omega)} \right|^2 \qquad (22)$$

A linearized form of the LSE is also used, as follows:

$$E = \sum_{\omega=\omega_1}^{\omega_2} \left| W_0(\omega)\left(H_m(\omega)A(\omega) - B(\omega)\right) \right|^2 \qquad (23)$$

where $W_0(\omega)$ is arbitrary weighting function. It is usually a first step in the nonlinear optimization problem (22).

After the estimation of the set of coefficients of polynomials $B(s)$ and $A(s)$, the poles and zeros calculation and partial fractional expansion to the form given by (3), the parameters of system resonances can be estimated (f_n, Q, ΔL).

The problem with a LSE transfer function identification in a s-domain is that it is numerically unstable, as LSE calculation exhibits sensitivity to coefficient a_k and b_k, that is proportional to k-th power of the frequency. A better approach is to make a transfer function identification in the discrete complex frequency z-domain. The transfer function in the z-domain, called the system function, is defined as:

$$H_d(z) = \frac{B(z^{-1})}{A(z^{-1})} = \frac{\sum_{i=0}^{m} b_i z^{-i}}{\sum_{k=0}^{n} a_k z^{-k}} = C \frac{\prod_{i=1}^{m}\left(1 - z_{zi}z^{-1}\right)}{\prod_{k=0}^{n}\left(1 - z_{pk}z^{-1}\right)} \qquad (24)$$

The first form of the $H_d(z)$ is a quotient of two polynomials $B(z^{-1})$ and $A(z^{-1})$ that are m-order and n-order power series of complex variable z^{-1}. The second form is factorised form with m zeros (z_{zi}, $i=0,1,..m$) and n poles poles (z_{pk}, $k=0,1,..n$) of the system function. The frequency response function $H(e^{jw})$ can be obtained by substituting $z=e^{jw}$, where $w=\omega T$ is normalized frequency and T is the sampling period. As the magnitude of $|(e^{jw})^{-k}|$ is always less than one, for every k, we get an equal numerical error sensitivity for all estimated coefficients.

The identification in the z-domain enables the application of simple iterative Steiglitz-McBride method for solving the nonlinear LSE problem. In that method, at k-th iterative step a linearized error function is being minimized:

$$E_k = \sum_{w=0}^{\pi} \left| W_k(e^{jw})\left(H_m\left(e^{jw}\right)A_k\left(e^{jw}\right) - B_k\left(e^{jw}\right)\right) \right|^2$$

where $\qquad\qquad\qquad\qquad\qquad\qquad (25)$

$$W_k(e^{jw}) = \begin{cases} W_0(e^{jw}), & for \quad k=0 \\ W_0(e^{jw})/A_{k-1}(e^{jw}), & for \quad k>0 \end{cases}$$

Forming of LSE matrices for the solution of this problem in the frequency domain is described in [8]. In the Matlab Signal processing toolbox [10] there is a version of this method that is defined in the time domain. There, the application of weighted function is realized as pre-filtering in the time domain, while identification starts with a linearized LSE Prony method [11].

The solution procedure in both cases is extended in this work with application of SVD numerical technique (singular value decomposition) to overdetermined LSE matrix for removal of poles that appeared to be by-products of the unwanted measurement noise. Unfortunately, that step was not sucessful in cases where the measured impulse response contained reflections.

The sequence of operations needed to obtain the parameters of system resonances is as follows:

1) Make measurement of impulse response with minimum influence of noise and reflections. For the measured impulse response determine the start sample as one that gives a response closest to minimum phase response.
2) Use the measured impulse response to estimate the equivalent discrete system (24) by using the nonlinear LSE method (25). For the reduction of system order apply the SVD technique on overdetermined LSE matrices. The result gives order and coefficients of system polynomials $B(z^{-1})$ and $A(z^{-1})$.
3) Calculate zeros and poles of the discrete transfer function.
4) Make a partial fraction expansion, and find the residuums of all complex conjugate poles.
5) Transform complex conjugate pole in z-domain into poles in s-domain and determine residuums. Use equation (2) and (3) to determine resonant frequency, Q-factor and level of every resonance.
6) Show results in tabular and graphic form.

As an example for this procedure the results of the estimation of resonance parameters for the high-frequency loudspeaker YAMAHA B26 are shown in Table 1.

f_r (Hz)	ΔL (dB)	Q-factor
1699,3	0,84	1,40
2409,1	4,11	1,69
3544,2	-17,71	4,33
4340,7	-11,72	2,98
8065,9	-4,19	2,81
11103,0	-17,57	7,71
12248,0	-7,11	7,83
14876,0	1,85	4,23
15830,0	-19,77	10,39
19743,0	-7,54	2,42
21204,0	-24,83	15,59

Table 1. Parameters of B26 tweeter resonances

Figure 14 shows the frequency response and the individual responses of resonances for that loudspeaker. Figure 15 shows the CSD and Fig. 16 shows the Burst decay for the same loudspeaker. It is obvious that CSD and Burst decay are inferior to the system identification method for detection of audible resonance. The transfer function identification gives all the necessary information to estimate audibility of resonances while CSD and Burst

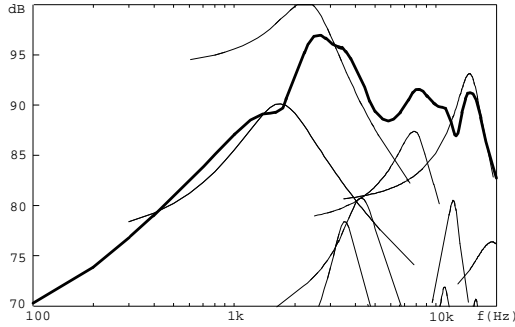decay only gives insight in the presence of resonances on some frequencies.

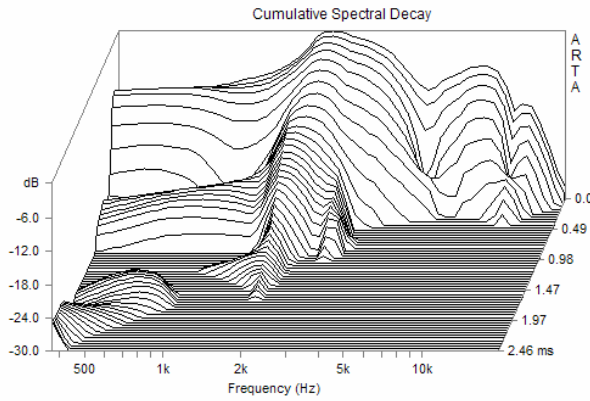**Fig. 14.** Frequency response and individual response of resonances for tweeter B26

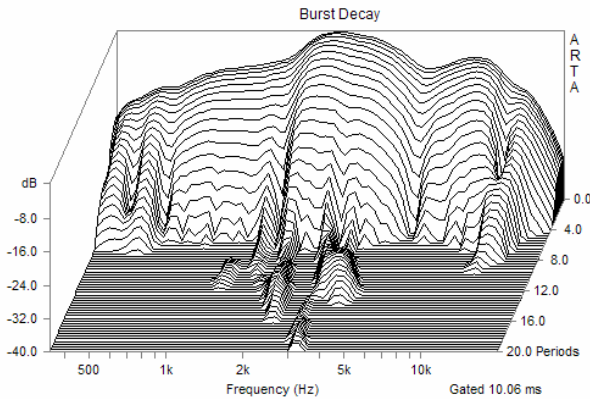**Fig. 15.** CSD of tweeter B26

Fig. 16. Burst decay of tweeter B26

Step 5) needs some more explanation. The problem is how to estimate the transfer function in *s*-domain from a known discrete transfer function of a equivalent system in *z*-domain. It is well known [11] that we can use impulse-invariant or step-invariant transformations. It depends on what type of AD/DA converters are used in the measurement of the impulse response.

The impulse invariant transformation between transfer function in the *s*-domain and system function in the *z*-domain is defined as:

$$H_d(z) = Z\{H(s)\} = \sum_k \left(\text{Res}\, H(s) \frac{1}{1 - e^{Ts}z^{-1}} \right)_{s \to s_{pk}} \quad (26)$$

The step invariant transformation accounts for the effects of the sample and hold circuit. It is defined by the following equation:

$$H_d(z) = Z\left\{ \frac{1 - e^{-sT}}{s} H(s) \right\} = \left(1 - z^{-1}\right) Z\left\{ \frac{H(s)}{s} \right\} \quad (27)$$

By specialization of expression (26) and (27) for cases of single and multiple real and conjugate complex poles, a table of transformation for partial fraction expansion terms from *z*-domain to *s*-domain is generated.

In practical realization of the transfer function identification the measurement noise makes that there are no multiple poles.

For both type of transformations the transformation of poles is the same;

$$z_{pk} = e^{s_{pk}T}, \quad s_{pk} = \frac{1}{T} \ln z_{pk}, \quad (28)$$

the only difference is in the transformation of residuums.

Older single-channel measurement systems, like MLSSA, mainly use multi-bit converters that have sample and hold units and analogue antialiasing filters. For that kind of converter a step invariant transformation should be used.

Modern converters are generally of sigma-delta type. In single channel measurement systems, which use sigma-delta converters, the measured transfer function contains the response of antialiasing filters. That filters are of FIR type and have very high orders (as result of 64-128 times oversampling). The ringing of these filters introduces a lot of resonances and makes identification impossible. Generally, we can expect good results if we have to identify systems with 40-50 resonances.

The better approach is to measure with a two channel Fourier analysers [4], with very high sampling rate and than make the low-order IIR filtering and down-sampling. For example, loudspeaker testing could be done with sampling frequency 192kHz, filtered with IIR filter that has all resonances above 20kHz and then make resampling to 48kHz. In this case the conversion from *z*-domain poles to *s*-domain poles should be done by the impulse invariant transformation.

The problem arises if there is an initial delay in the impulse response. Numerically, LSE method tries to compensate delays by introducing series of all-pass filters, each one with one pole and one zero. That lowers the LSE numerical resolution. It is advisable that the start

of the impulse response is to be set close to the start of the equivalent minimum phase system.

7. CONCLUSION

The detection of resonances is very important in audio system design. Fryer [1] and Floyd [2] have established criteria for the evaluation of resonance's threshold of audibility. Following their work, this paper shows that three parameters needed for judging the audibility of resonances are resonant frequency, Q-factor and the level of resonances below the system response. It is shown that these parameters define the energy of the resonance, which seems to be proportional to the resonance loudness.

Resonances can be detected from frequency response curves, from group delay curves, from loudspeaker impedance, from changes of the level of harmonic distortions, from CSD waterfall and sonogram graphs and from envelope of the burst decay. All these measurement are reliable only for the estimation of one parameter: the natural frequency of the resonance. The level and the Q-factor of the resonance can be detected from these curves only partially and requires an experienced operator.

The burst decay envelope is obtained by Morlet wavelet transform. That gives the burst decay presentation with optimal time bandwidth product. The burst decay graphs are shown in a period based scale. This enables the presentation of resonances with a same Q-factor also with equal decay pattern over all audio frequencies. These two characteristics give advanced features to the burst decay graph for visualization of system resonances.

The best method for the detection of resonances is by using the transfer function identification. It delivers all resonance parameters from complex conjugate poles and residuums of the partial fraction expansion of the transfer function.

The Steiglitz-McBride nonlinear LSE method was reliably used to make identification of systems that has more than fifty resonances. The quality of the identification procedure depends on three factors: noise level, existence of reflections and the determination of the impulse response starting sample position. For best results the measurement would be done in an anechoic environment and starting sample position would be determined so that impulse response is as close as possible to the equivalent response of the minimum phase system.

The SVD numerical technique is used to determine lowest possible system order. It was found that SVD technique is effective only if the measured impulse response does not contain reflected energy.

The conversion system function in z-domain to transfer function in s-domain would be done by step invariant transformation if the measurement is done with a single channel system that has multi-bit converters and analogue antialiasing filters. Otherwise, in systems that uses sigma-delta converters it is necessary to use a dual channel measurement with a high sampling rate, followed by down-sampling and IIR antialiasing filtering. For such systems, the conversion from z-domain to s-domain should be done by the impulse-invariant transformation.

For all presented methods for detection of resonances one thing is common: if the system response contains reflected energy many resonances, especially those with low Q-factor, are undetectable. This means that for meaningful application of presented methods the measurement of the impulse response has to be made in an anechoic environment, or gating technique can be used to remove part of impulse response that cantain reflections.

REFERENCES

[1] P. A. Fryer: **Loudspeaker Distortions, Can We Hear Them**, Hi-Fi News Rec. Rev., vol. 22, June, 1997, 51-56

[2] F. E. Toole, S. R. Olive: **The Modification of Timbre by Resonances: Perception and Measurement**, *JAES*, vol. 32, March, 1988, 122-142

[3] B. C. J. Moore, *An Introduction to the Psychology of Hearing*, Academic Press, 1997.

[4] I. Mateljan: ***ARTA, Program for real-time audio analysis - User Manual ver. 1.3.0***, ARTALABS, 2007.

[5] J. D. Bunton, R.Small: **Cumulative Spectra, Tone Burst and Apodization**, *JAES*, vol. 26, July, 1982.

[6] S. Linkwitz: **Shaped Tone-Burst Testing**, *JAES*, Vol. 28, No. 4, April 1980.

[7] D. B. Keele: **Time-Frequency Display of Electroacoustics Data Using Cycle-Octave Wavelet Transforms**, *AES 99 Convention*, New York, October, 1999.

[8] I. Mateljan: **Impulse Measurement System Identification,** 13th *International Congress on Acoustics*, vol.4. Beograd, 1989. 85-89

[9] K. Steiglitz, L. E. McBride: **A technique for the identification of linear systems,** *IEEE Trans. Automatition Control*, vol.AC-10, 1965, 461-464

[10] User's Guide, ***Signal Processing Toolbox for MatLab***, Version 5, Parametric Modeling, 2000.

[11] J. G. Proakis, D. G. Manolakis, ***Digital Signal Processing, Principles, Algorithms, and Applications***, Third Edition, Prentice Hall, Upper Saddle River, NJ, 1996.

[12] D. D. Rife: ***MLSSA Reference Manual***, DRA Laboratories, 10WI-4, 2001.